

## Magnetization Transfer Contrast (MTC) and Tissue Water Proton Relaxation *in Vivo*

STEVEN D. WOLFF\* AND ROBERT S. BALABAN†

Laboratory of Cardiac Energetics, National Heart Lung and Blood Institute, Bethesda, Maryland 20892

Received November 4, 1988; revised December 30, 1988

In this study the exchange between  $^1\text{H}$  magnetization in "free" water ( $^1\text{H}_f$ ) and that in a pool with restricted motion ( $^1\text{H}_r$ ) was observed in tissues *in vivo* using NMR saturation transfer methods. Exchange between these two pools was demonstrated by a decrease in the steady-state magnetization and relaxation times of  $^1\text{H}_r$  with radiofrequency irradiation of  $^1\text{H}_r$ . The pseudo-first-order rate constant for the movement of magnetization from  $^1\text{H}_r$  to  $^1\text{H}_f$  was  $\sim 1 \text{ s}^{-1}$  in kidney and  $\sim 3 \text{ s}^{-1}$  in skeletal muscle *in vivo*. Proton NMR imaging demonstrated that this exchange was tissue specific and generated a novel form of NMR image contrast. The extent of exchange between  $^1\text{H}_f$  and  $^1\text{H}_r$  as well as the topological correlation of the exchange with relaxation weighted images suggests that this pathway is a major determinant of the observed relaxation properties of water  $^1\text{H}$  *in vivo*. © 1989 Academic Press, Inc.

### INTRODUCTION

The relaxation properties of water  $^1\text{H}$  nuclei are the basis for most of the contrast obtained by nuclear magnetic resonance (NMR) imaging techniques. Conventional  $^1\text{H}$  NMR images of biological tissues usually reflect a combination of spin-lattice ( $T_1$ ) and spin-spin ( $T_2$ ) water  $^1\text{H}$  relaxation. The variations in water  $^1\text{H}$  relaxation rate generate image contrast between different tissues and pathologies depending on how the NMR image is collected. While the general mechanisms for water  $^1\text{H}$  relaxation have been described (1), the precise nature of these relaxation processes in tissue is still an active area of research. Investigators have proposed that a predominant relaxation mechanism in biological tissue is cross-relaxation and/or chemical exchange between  $^1\text{H}$  in "free" or highly mobile water and  $^1\text{H}$  associated with macromolecules or immobile water (2-6). These conclusions were based on detailed studies of the effect of static magnetic field strength (5, 6) as well as selective and nonselective excitation pulses (2-4) on water  $^1\text{H}$  relaxation rates.

The purpose of this study was to measure the rate of magnetization exchange between  $^1\text{H}$  spins in "free" water ( $^1\text{H}_f$ ) and  $^1\text{H}$  spins in regions of restricted motion ( $^1\text{H}_r$ ) as well as to image the distribution of this exchange process in intact tissues. To accomplish this, we used the saturation transfer method originally described by Forsen and Hoffman (7) in which the rate of magnetization exchange between two

\* Howard Hughes Medical Institute-NIH Research Scholar.

† To whom correspondence should be addressed.

pools can be quantitatively measured. This technique has been used extensively to measure chemical exchange rates in intact tissues (8-10). Saturation transfer involves the selective steady-state irradiation, with radiofrequency energy, of one member of an exchanging pair of spins and observation of the effects of this irradiation on its nonirradiated exchange partner. If exchange is occurring, the irradiation will cause a decrease in the steady-state magnetization and a decrease in the observed  $T_1$  of the nonirradiated spin (8, 11). These effects are not limited to chemical exchange, since through-space cross-relaxation between the two pools will have identical effects.

#### MATERIALS AND METHODS

All experiments were performed using General Electric CSI spectrometers operating at 4.7 or 2.0 T. The rabbit kidney and skeletal muscle preparations were used as previously described (9, 10, 12). Coil designs for these studies were also previously described for the rabbit leg (9) and kidney (12) *in vivo*.

#### RESULTS

Saturation transfer experiments were performed in the present study by irradiating the immobilized  $^1\text{H}_r$  pool and observing the effect on the steady-state magnetization as well as the observed spin-lattice relaxation ( $T_1$ ) time of  $^1\text{H}_r$ . We assumed that radiofrequency irradiation  $\geq 5$  kHz from the  $^1\text{H}_r$  resonance would result in a selective irradiation of  $^1\text{H}_r$ , since  $^1\text{H}_r$  would have an NMR linewidth much greater than  $^1\text{H}_f$  (i.e., the  $T_2$  relaxation time should be shorter for  $^1\text{H}_r$ ) (13). Saturation transfer experiments were conducted by preirradiating at frequencies selected within 200 kHz of the Larmor frequency of the  $^1\text{H}_r$  resonance. Figure 1 shows the effect of irradiation at the frequency 10 kHz lower than the  $^1\text{H}_r$  resonance of a rabbit kidney *in vivo*. The preirradiation resulted in a specific 30% decrease in the magnitude of the water resonance (measured as the area of the resonance peak) that was not observed for the other  $^1\text{H}$  signals from fats or trimethylamines even though the irradiation was closer in frequency to these metabolites. This effect was also reproduced in rabbit skeletal muscle and brain *in vivo*. These results are consistent with the presence of a specific magnetization exchange between  $^1\text{H}_f$  and  $^1\text{H}_r$  pools in these tissues.

The decrease in  $^1\text{H}_f$  signal by irradiation of  $^1\text{H}_r$  was found to be power- and frequency-dependent. The effect of irradiation power on the steady-state  $^1\text{H}_f$  signal is shown in Fig. 2A. Using this curve, the maximum decrease in steady-state  $^1\text{H}_f$  magnetization obtained by irradiating  $^1\text{H}_r$  was estimated to be 70% in the kidney *in vivo*. This irradiation power versus  $^1\text{H}_f$  magnitude curve was obtained for all of the tissues and fluids studied in this investigation to assure that a maximum effect of irradiation was recorded at any given frequency.

A significant decrease in the net magnetization of the  $^1\text{H}_f$  resonance was observed over a wide range of irradiation frequencies ( $\pm 50$  kHz) surrounding its resonance frequency. The effect of different irradiation frequencies, at constant power (0.4 W), is shown in Fig. 2B. The linewidth of the irradiation effect was approximately 40 kHz and symmetrically centered around the  $^1\text{H}_f$  resonance in the rabbit kidney (Fig. 2B) and skeletal muscle *in vivo* (not shown) as well as in canine heart muscle *in vitro* (Fig. 2C). No magnetization transfer was observed in distilled water (Fig. 2B), manganese-

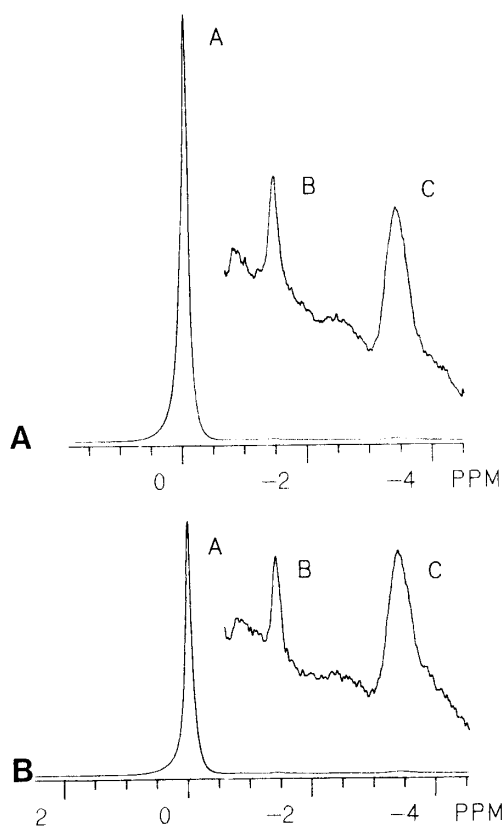


FIG. 1. Effect of preirradiation on  $^1\text{H}$  NMR detected metabolites and water of the rabbit kidney *in vivo*. The rabbit kidney preparation and NMR probe design were previously described (12). The animal's temperature was maintained at  $37^\circ\text{C}$ . Each spectrum resulted from 16 averages of a  $\pi/2-\tau-\pi-\tau$ -acquire sequence in which  $\tau = 50$  ms. For this study the magnetic field strength was 4.7 T. Complex points (1K) were collected with an acquisition time of 256 ms. (A) Without preirradiation, interpulse delay = 6 s. (B) With preirradiation (0.4 W, 10 kHz below the  $^1\text{H}_r$  resonance frequency) during the last 4 s of the interpulse delay. Peak assignments are (A) water, (B) trimethylamines, and (C) lipids.

doped water samples (to mimic *in vivo*  $T_2$  values), or rabbit urine samples (not shown). The bandwidth (in Hz) of this effect was found to be independent of magnetic field strength (4.7 and 2 T) in canine heart muscle *in vitro* (Fig. 2C) and was equivalent to that found in 3% agar solutions (not shown). The field independence of the linewidth suggests that the restricted motion of this  $^1\text{H}_r$  pool approaches the rigid-lattice condition (correlation time  $> 10^{-7}$  s $^{-1}$ ) (13).

The effect of nonspecific radiofrequency bleed over from an irradiation is usually controlled by irradiating frequencies on either side of a specific resonance to look for frequency-specific effects (8-10). Since the  $^1\text{H}_r$  component is symmetrical around  $^1\text{H}_f$  (Figs. 2B and 2C) such controls are not possible in these experiments. However, the radiofrequency bleed from the off-resonance irradiation can be determined using the equation (14)

$$M_s = M_0(1 + T_{2f}^2\omega^2)/(1 + T_{2f}^2\omega^2 + \gamma^2 H_1^2 T_{1f} T_{2f}), \quad [1]$$

where  $\omega$  is the offset frequency (hertz),  $\gamma$  is the gyromagnetic ratio, and  $H_1$  is the magnetic field (tesla) induced by the irradiation. For this calculation, it is assumed

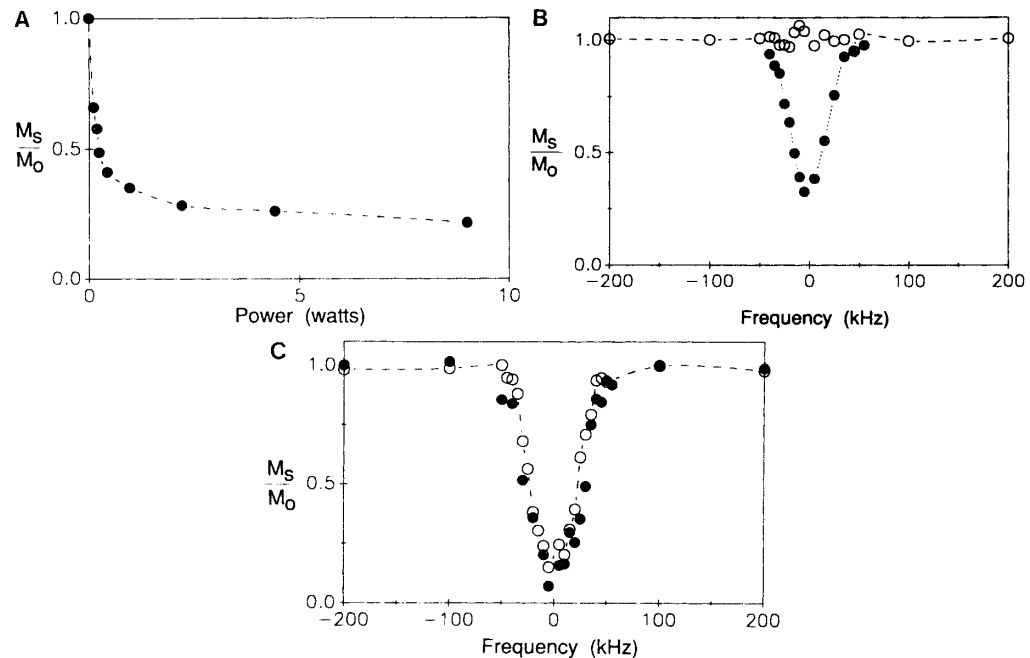


FIG. 2. (A) Effect of preirradiation power on the magnitude of the water resonance of the rabbit kidney *in vivo*. Preparation was identical to that used in Fig. 1. Spectra were acquired from a  $\pi/8$  pulse that followed a 6-s interpulse delay where during the last 4 s there was rf preirradiation 5 kHz below the  $^1\text{H}_f$  resonance frequency. Field strength was 4.7 T. (B) Effect of preirradiation frequency on the magnitude of the  $^1\text{H}_f$  resonance from the rabbit kidney *in vivo* (●) and distilled water (○). Spectra were collected with a  $\pi/8$ -acquire pulse sequence with no echo in this case. Preirradiation power was 0.4 W. Field strength was 4.7 T. The *in vivo* kidney was the same preparation as that described in Fig. 1. The distilled water sample (25°C) in a glass tube was placed in the same coil as that used to collect the kidney data. The  $^1\text{H}_f$  resonance frequency is at 0 Hz. Only data collected with the irradiation > 5 kHz off of the  $^1\text{H}_f$  resonance are reported to minimize the effects of radiofrequency "bleed over." (C) Effect of preirradiation frequency on the magnitude of the  $^1\text{H}_f$  resonance of canine cardiac tissue at two field strengths. Approximately 2 g of excised canine left ventricle muscle was placed in a glass tube and inserted into an NMR probe which could be tuned to the Larmor frequency of  $^1\text{H}$  at the two fields. The temperature of these samples was 25°C. Spectra were collected as described in (A). (●) *Ex vivo* myocardium at 2.0 T. (○) Same tissue at 4.7 T.

that the irradiation time is on the order of  $T_{1f}$ . Other terms are defined in the text. The  $H_1$  fields were estimated by determining the time required to produce a  $360^\circ$  flip by the decoupler at the power levels used in this study. The  $H_1$  field varied from  $7.0 \times 10^{-6}$  T (0.4 W) to  $3.5 \times 10^{-5}$  T (8 W) in the kidney coil and  $6 \times 10^{-6}$  T (0.75 W) to  $1.6 \times 10^{-5}$  T (4.4 W) in the leg coil. Using an irradiation strength of  $7 \times 10^{-6}$  T at 5 kHz (which was used for the rate constant calculations in this study), a  $T_{2f}$  of 60 ms determined from spin-echo experiments, and a  $T_{1f}$  of 1.5 s (see Table 1), the bleed over of radiofrequency energy would result only in a <8% decrease in the  $^1\text{H}_f$  resonance of the kidney. Thus, the irradiation effects observed in this study can be only minimally influenced by radiofrequency bleed over. The  $T_2$  of  $^1\text{H}_f$  ( $T_{2f}$ ) can be estimated from the frequency plot shown in Figs. 2B and 2C using Eq. [1] which can be used to define the frequency response of the irradiation as a function of power,  $T_1$  and  $T_2$ . The irradiation  $H_1$  field was  $7 \times 10^{-6}$  T and a  $T_{1f}$  of 1 s was assumed (on the

TABLE I  
Effect of  $^1\text{H}_r$  Saturation *in Vivo*

Tissue	$T_{1\text{fobs}}$ (s)	$T_{1\text{fsat}}$ (s)	$M_s/M_0$	$T_{1f}$ (s)	$k_a$ ( $\text{s}^{-1}$ )	$N$
Kidney	$1.5 \pm 0.05$	$0.62 \pm 0.08$	$0.30 \pm 0.03$	$2.0 \pm 0.2$	$1.2 \pm 0.2$	4
Skeletal muscle	$1.5 \pm 0.02$	$0.30 \pm 0.03$	$0.07 \pm 0.005$	$4.5 \pm 0.5$	$3.1 \pm 0.3$	4

Note. All experiments were conducted on rabbits *in vivo* at 4.7 T and 37°C.  $T_{1\text{fobs}}$  and  $T_{1\text{fsat}}$  were determined using an inversion recovery experiment as previously described for  $^{31}\text{P}$  in skeletal muscle (10) to obtain uniform times of saturation. For the kidney irradiation, 0.4 W was used to obtain saturation for the  $T_{1\text{fsat}}$  and  $M_s/M_0$  determinations. For skeletal muscle irradiation, 1.6 W was used. All terms are defined in the text.  $T_{1f}$  and  $k_a$  were calculated using Eqs. [2] and [3], respectively. All data are presented as means  $\pm$  standard error of the mean.

basis of the estimated correlation time of this dipolar spin). This resulted in a calculated  $T_{2r}$  of 0.2 ms assuming that the  $H_1$  field was uniform as a function of frequency with these rather low  $Q$  ( $\sim 90$ ) loaded coils.

The  $T_1$  of the  $^1\text{H}_f$  pool in the absence of exchange ( $T_{1f}$ ) can be determined from the effect of  $^1\text{H}_r$  irradiation on the observed  $T_1$  of the  $^1\text{H}_f$  pool ( $T_{1\text{sat}}$ ) and the steady-state  $^1\text{H}_f$  magnetization before ( $M_0$ ) and after ( $M_s$ ) irradiation according to the following equation for an inversion recovery experiment (11),

$$T_{1f} = M_0/M_s \times T_{1\text{sat}}, \quad [2]$$

where  $M_0$  is the  $^1\text{H}_f$  steady-state magnetization without irradiation and  $M_s$  is with irradiation of  $^1\text{H}_r$ . It should be noted that  $T_{1f}$  will still be influenced by other  $T_1$  relaxation mechanisms, such as exchange with  $^1\text{H}$  pools not irradiated and/or paramagnetic relaxation. To evaluate the effect of  $^1\text{H}_r$  irradiation on the observed  $T_1$  of  $^1\text{H}_f$ , inversion recovery experiments were conducted in the presence and absence of irradiation of the  $^1\text{H}_r$  pool. With a 0.4-W irradiation 5 kHz from the  $^1\text{H}_f$  resonance, the  $T_1$  changed from  $\sim 1.5$  s without irradiation to  $\sim 0.62$  s. This observed decrease in the  $T_1$  of  $^1\text{H}_f$  with irradiation of  $^1\text{H}_r$  is also consistent with the exchange of magnetization between these two pools. Using Eq. [2], the  $T_{1f}$  values of whole kidney and rabbit skeletal muscle were calculated and are presented in Table 1. The  $T_{1f}$  of the kidney ( $\sim 2$  s) is much shorter than that of skeletal muscle ( $\sim 4.5$  s) implying that a  $T_1$  relaxation mechanism other than magnetization exchange with the  $^1\text{H}_r$  pool is affecting the  $^1\text{H}_f$  pool in kidney. Likely candidates for this additional relaxation effect in kidney are paramagnetic metals, such as manganese, which are 10 times higher in concentration in kidney than in skeletal muscle (15).

The apparent pseudo-first-order rate constant for the movement of magnetization from  $^1\text{H}_f$  to  $^1\text{H}_r$  can be estimated from the effects of irradiating  $^1\text{H}_r$  on the  $^1\text{H}_f$  pool  $T_1$  and steady-state magnetization using the equation (7-10)

$$k_a = 1/T_{1\text{sat}}[1 - M_s/M_0], \quad [3]$$

where  $k_a$  is the apparent pseudo-first-order rate constant of magnetization transfer from  $^1\text{H}_f$  to  $^1\text{H}_r$ . Table 1 lists the calculated  $k_a$  values for rabbit skeletal muscle and

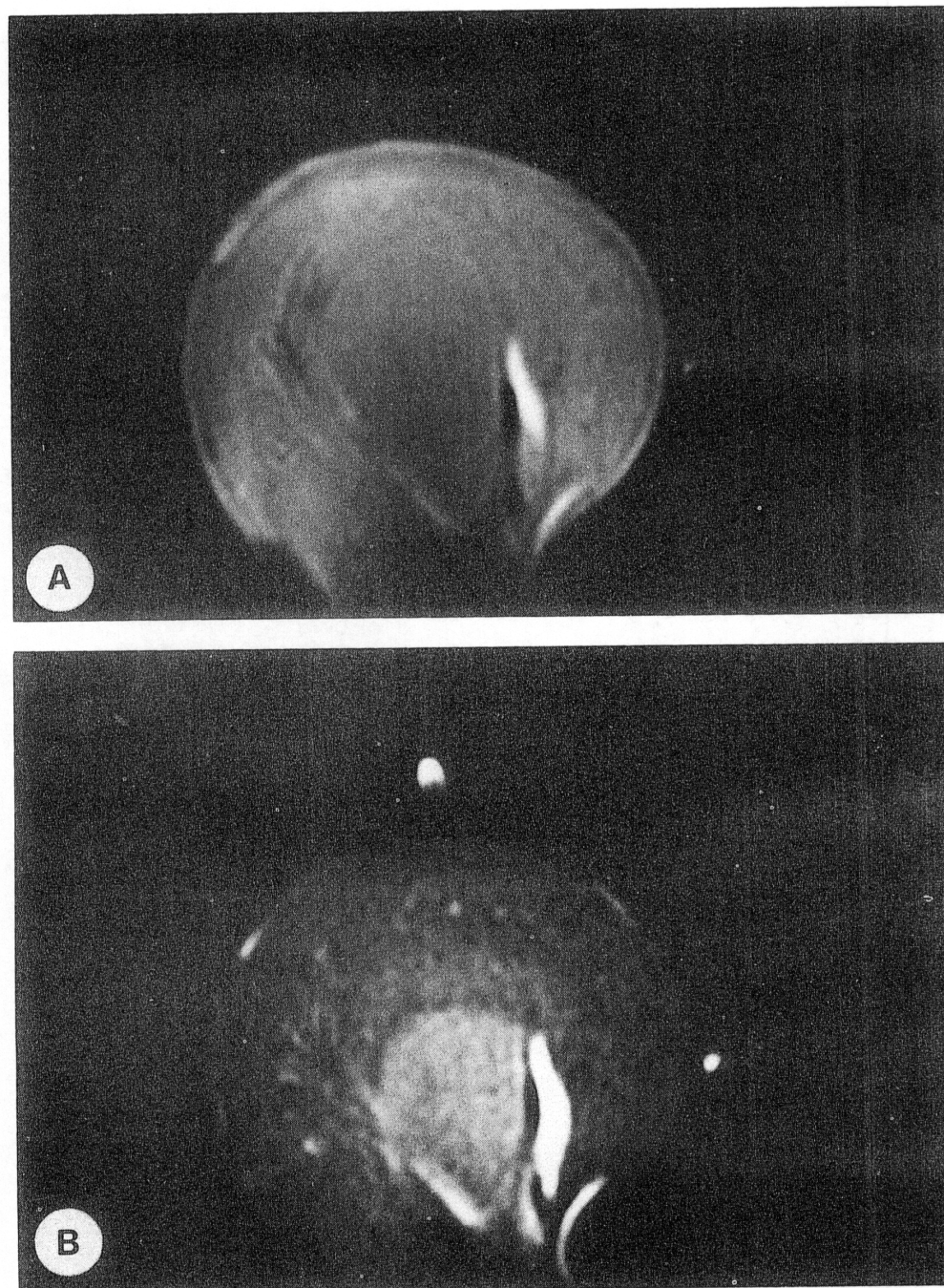


FIG. 3. Transverse spin-warp  $^1\text{H}$  NMR images of rabbit kidney *in vivo*. The rabbit kidney preparation was as previously described (12). (A)  $^1\text{H}$  density image, TR = 4.2 s, TE = 20 ms, field of view =  $40 \times 40 \times 3$  mm, digital matrix size  $128 \times 128$ . (B) Image collected using the same parameters as above, but with 3.5 s of 0.4 W irradiation 5 kHz below the resonance frequency of  $^1\text{H}$  occurring just before slice selection. (C) Ratio image of image (B) divided by image (A) ( $M_s/M_0$  image). (D)  $T_2$ -weighted kidney image. Collection conditions are the same as those in (A) only an 80-ms TE is used to generate  $T_2$  contrast.

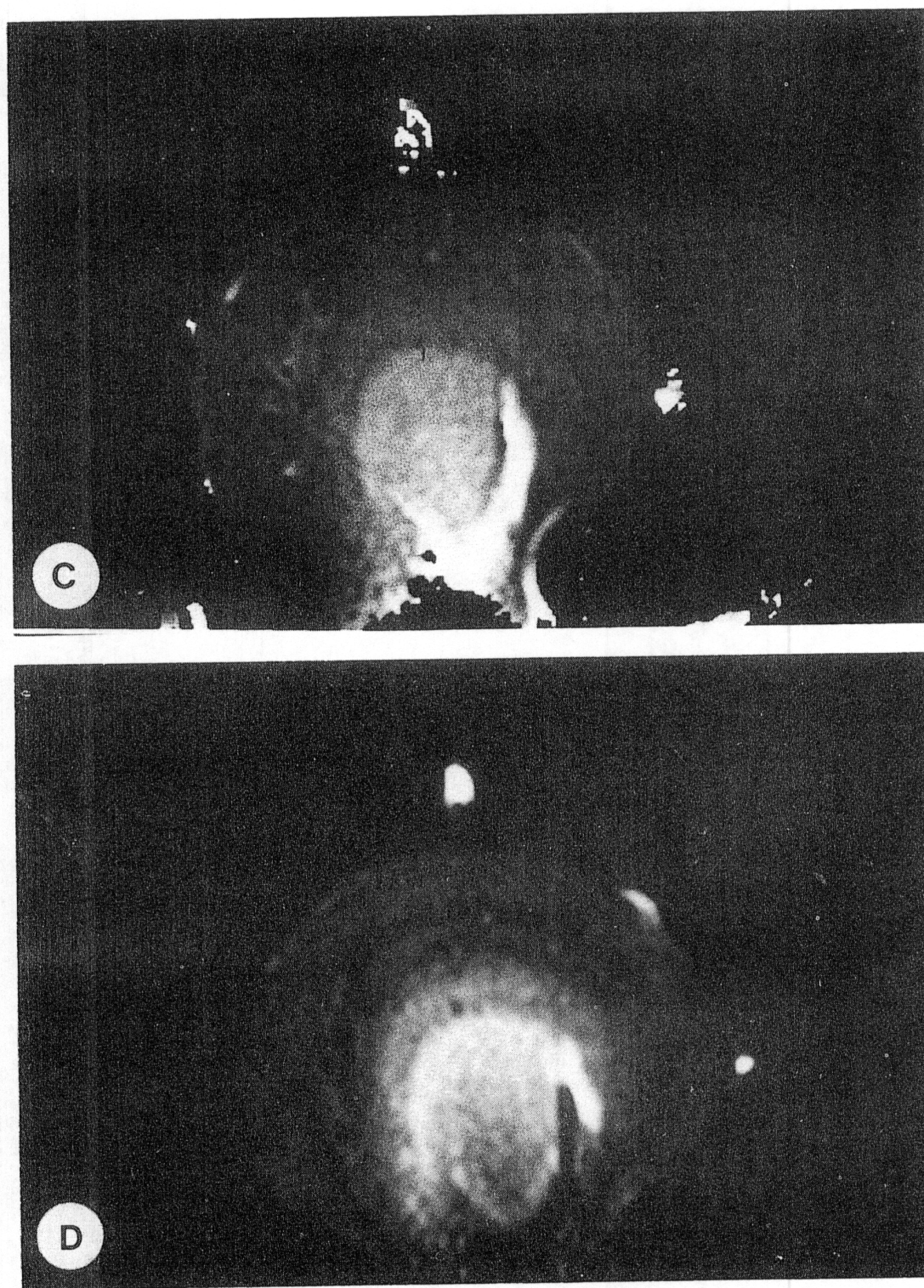


FIG. 3—Continued

kidney *in vivo* using Eq. [3]. The higher rate constant in skeletal muscle may be due to a higher protein content and/or a more efficient exchange mechanism in this tissue.

The values presented in Table 1 represent the average exchange occurring over the whole tissue studied. To investigate whether or not this magnetization exchange between  $^1\text{H}_f$  and  $^1\text{H}_r$  is homogeneous throughout tissues, the effect of  $^1\text{H}_r$  irradiation on the distribution of steady-state  $^1\text{H}$  magnetization was evaluated using NMR  $^1\text{H}$

imaging. Since the conventional NMR imaging experiment requires the collection of an echo, these techniques generally detect only the  ${}^1\text{H}_f$  pool because of its relatively long  $T_2$ . NMR images of the kidney *in vivo* were taken using a conventional spin-warp sequence with and without irradiation 10 kHz from  ${}^1\text{H}_f$  resonance. The images presented in Figs. 3A and 3B were collected with a 4.2-s recycle time (TR) and 20-ms echo time (TE) to minimize  $T_1$  and  $T_2$  contrast effects. Figure 3A is the control image without irradiation, Fig. 3B is with irradiation, and Fig. 3C is the ratio of irradiated image to the control image (i.e., an  $M_s/M_0$  image (9)). To obtain an actual  $k_a$  image, the  $T_{\text{1sat}}$  of each voxel would have to be determined (9). The intensity of the renal cortex of the kidney was reduced by the irradiation to a much greater extent than the inner medulla resulting in improved contrast between these regions in the irradiated image (Fig. 3B) as well as the ratio image (Fig. 3C). This suggests that the exchange rate in the cortex of the kidney is higher than that in the inner medulla. The urine, blood vessels, and fat were not significantly affected by the irradiation resulting in a very high intensity signal from these structures in the irradiated (Fig. 3B) and ratio (Fig. 3C) image. The lack of effect on urine presumably is due to the limited number of macromolecules in urine resulting in limited magnetization exchange between a  ${}^1\text{H}_r$  and a  ${}^1\text{H}_f$  pool. Blood  ${}^1\text{H}_f$  was less affected by irradiation since the flow of blood results in  ${}^1\text{H}$  spins entering the field of view which were not irradiated if they came from a region outside of the coil. Furthermore, the irradiation of  ${}^1\text{H}_r$  in whole rabbit blood (hematocrit 43%) *in vitro* resulted in a decrease in  ${}^1\text{H}_f$  which was approximately twofold less than that of the whole kidney, indicating that the  ${}^1\text{H}_f$ - ${}^1\text{H}_r$  exchange is relatively slow in blood. The fat was unaffected since this resonance does not exchange with the  ${}^1\text{H}_r$  component (Fig. 1). These results demonstrate that the magnitude of the irradiation effect on  ${}^1\text{H}_f$  is tissue specific and causes tissue contrast in the NMR image on the basis of the exchange process as well as flow from regions not affected by the irradiation.

#### DISCUSSION

These data demonstrate that the  ${}^1\text{H}_f$  pool is exchanging magnetization with an immobilized  ${}^1\text{H}_r$  pool. On the basis of the present data it is not possible to establish what portion of this exchange is due to a chemical exchange of protons or a through space interaction with immobilized water and/or macromolecules. Preliminary studies ( $n = 3$ ) with natural abundance or isotopically enriched  ${}^2\text{H}$  water signals in rabbit skeletal muscle *in vivo* reveal that no saturation transfer is observed with a broad component using conditions similar to those outlined for  ${}^1\text{H}$ . This result may imply that the dipolar cross-relaxation may be the dominant factor in the saturation transfer observed with  ${}^1\text{H}$ . However, the quadrupolar relaxation of  ${}^2\text{H}$  could result in such a broad line for the immobilized water that it could not be effectively saturated in these protocols and/or the relaxation processes could simply be dominated by the quadrupolar relaxation process. Clearly, more studies are required to establish the actual mechanism causing the saturation transfer observed between  ${}^1\text{H}_f$  and  ${}^1\text{H}_r$ .

Independent of the mechanism, the exchange between the  ${}^1\text{H}_f$  and the  ${}^1\text{H}_r$  pool will result in the observed  ${}^1\text{H}_f$  relaxation times (i.e., both  $T_1$  and  $T_2$ ) to be affected by the relaxation times of the  ${}^1\text{H}_r$  pool according to the equation



$$1/T_{\text{fobs}} = 1/T_f + X_r/(T_r + 1/k_r), \quad [4]$$

where  $T_{\text{fobs}}$  is the observed  $T_1$  or  $T_2$  of the  $^1\text{H}_f$  pool,  $T_f$  is the  $T_1$  or  $T_2$  of the  $^1\text{H}_f$  pool in the absence of exchange,  $X_r$  is the mole fraction of the  $^1\text{H}_r$  pool,  $T_r$  is the  $T_1$  or  $T_2$  of the  $^1\text{H}_r$  pool in the absence of exchange, and  $k_r$  is the rate constant of the transfer of magnetization from the  $^1\text{H}_r$  to the  $^1\text{H}_f$  pool. This equation is valid only when the two exchanging pools have the same chemical shift (see Fig. 2B) and  $X_r$  is less than 0.3 (13). With the  $^1\text{H}_f$  pool effectively at the rigid lattice condition, the  $T_2$  of this component will be much shorter than  $T_1$  (13). Thus, according to Eq. [4], we might expect the effect of the magnetization exchange to be much more pronounced for the observed  $T_2$  of the  $^1\text{H}_f$  pool than for its  $T_1$ . Indeed, the  $M_s/M_0$  images obtained for the rabbit kidney (Fig. 3C) and cat head (not shown) correlate with conventional  $T_2$ -weighted images (Fig. 3D) and not  $T_1$ -weighted images with regard to overall tissue contrast patterns. This latter result suggests that the pathway of relaxation through  $^1\text{H}_r$  is very significant in determining the observed  $T_2$  in these tissues.

The imaging technique described generates tissue contrast on the basis of the extent of magnetization transfer occurring in the tissue (i.e., magnetization transfer contrast (MTC)). This contrast is very similar, on a gross level, to  $T_2$  contrast although it can be obtained without long echo times. Indeed, we have been successful in obtaining high-contrast images using gradient-recalled echo sequences (5-ms TE) using this approach (Wolff and Balaban, in preparation).

In summary, it has been demonstrated in a variety of biological tissues that the free water component of the  $^1\text{H}$  NMR signal is in magnetization exchange with a relatively immobile component. The pseudo-first-order rate constant of this exchange varied from 0 to  $\sim 4 \text{ s}^{-1}$  depending on the particular tissue or fluid type. The exchange mechanism could include chemical exchange and/or cross-relaxation processes between the free water  $^1\text{H}$  and the  $^1\text{H}$  in or associated with large cellular macromolecules (proteins, membranes, etc.). The magnitude of this exchange process was imaged in tissue and provided a unique quantitative form of contrast for NMR imaging. Since the image contrast generated using this method is specific to the exchange between  $^1\text{H}_f$  and  $^1\text{H}_r$ , this technique may prove valuable in diagnosis or characterization of cancer, edema, or other pathologies where the specific relaxation mechanism may be useful in determining the nature of the disease.

#### ACKNOWLEDGMENTS

The authors thank the following investigators for numerous helpful discussions during the course of these experiments: Drs. B. Bryant, T. Brown, S. Konig, J. Alger, J. Eng, and B. Berkowitz.

#### REFERENCES

1. B. M. FUNG, "Methods in Enzymology," Vol. 127, p. 151, Academic Press, New York, 1986.
2. H. T. EDZES AND R. T. SAMULSKI, *Nature (London)* **265**, 521 (1977).
3. H. T. EDZES AND R. T. SAMULSKI, *J. Magn. Reson.* **31**, 207 (1978).
4. W. T. SOBOL, I. G. CAMERON, W. R. INCH, AND M. M. PINTAR, *Biophys. J.* **50**, 181 (1986).

5. S. H. KOENIG, in "Water in Polymers" (S. P. Rowand, Ed.), p. 157. American Chemical Society, Washington, DC, 1980.
6. S. H. KOENIG AND R. BROWN, in "NMR Spectroscopy of Cells and Organisms" (R. K. Gupta, Ed.), Vol. 2, p. 75, CRC Press, Boca Raton, FL, 1987.
7. S. FORSEN AND R. A. HOFFMAN, *J. Chem. Phys.* **39**, 2892 (1963).
8. J. R. ALGER AND R. G. SHULMAN, *Q. Rev. Biophys.* **17**, 83 (1984).
9. P. S. HSIEH AND R. S. BALABAN, *J. Magn. Reson.* **74**, 574 (1987).
10. P. S. HSIEH AND R. S. BALABAN, *Magn. Reson. Med.* **7**, 56 (1988).
11. B. E. MANN, *J. Magn. Reson.* **25**, 91 (1977).
12. S. D. WOLFF AND R. S. BALABAN, *J. Magn. Reson.* **75**, 190 (1987).
13. R. A. DWEK, "Nuclear Magnetic Resonance in Biochemistry," p. 40, Clarendon Press, Oxford, 1973.
14. A. CARRINGTON AND A. D. MCLACHLAN, in "Introduction to Magnetic Resonance: With Applications to Chemistry and Chemical Physics," p. 181, Harper & Row, New York, 1967.
15. H. FORE AND R. A. MORTON, *Biochem. J.* **51**, 600 (1956).